

CONTRIBUTION OF MRI IN LUNG CANCER STAGING*

A. Khalil^{1,2}, T. Bouhela¹, M.-F. Carette^{1,3}

Major advances in the WB-MRI in the initial evaluation and follow-up of patients with lung cancer have been performed in recent years. Multicentric studies using different magnet systems are necessary to confirm these promising results.

Key-word: Lung neoplasms, MR.

Lung cancer is the leading cause of cancer-related death worldwide, with a dismal 5-year survival rate of 15% (1). It accounts for 12.2% of all new cases of cancer in Europe in 2008 (1) and 14% of all new cases of cancer in the USA in 2011 (2). Accurate staging is mandatory to select the most appropriate therapy and to determine prognosis.

The two advanced imaging methods used for this staging were CT-scan and ¹⁸F-FDG PET/CT. However, both techniques had some limitations. Limitations of ¹⁸F-FDG PET/CT are particularly limited spatial resolution (3) and low specificity in distinguishing malignant nodule or lymphadenopathy from inflammatory changes, resulting in a considerable number of false-positive findings (4). The ¹⁸F-FDG PET/CT is not recommended for brain staging. Moreover, PET/CT is associated with a considerable radiation burden to patients and medical personnel. Limitations of CT-scan are the use of morphological (aspect and size of the nodule, size of the small diameter of the lymphadenopathy) data without functional or biological information.

Magnetic resonance imaging (MRI) is currently the only technique that enables non-invasive whole-body assessment without ionizing radiation. Another strength of MRI is its capability to create high soft tissue contrast without external contrast agents and with high spatial resolution. Currently, MRI is recommended in the assessment of lung cancer extension to the lung apices (superior sulcus or Pancoast-Tobias tumor), to the spinal cord, and to the cardiac cavity. For metastases issues, MRI is also recommended for its high sensitivity and specificity for brain, bone, liver and adrenal metastases diagnosis. Recent advances in

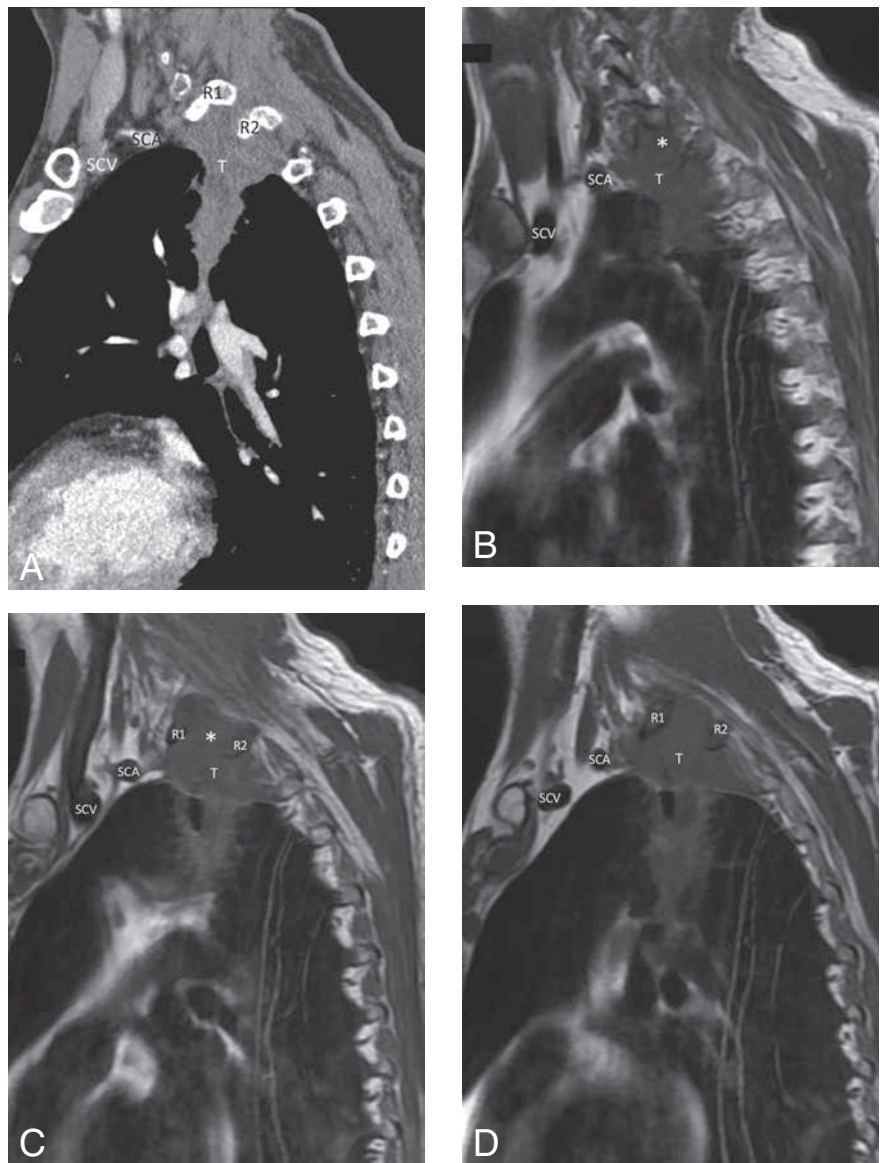


Fig. 1. — Left superior sulcus tumor. A: Multidetector CT-scan's sagittal reformatting shows the tumor invades the first (R1) and second (R2) ribs. The vascular structures, subclavian artery (SCA) and the subclavian vein (SCV), are not invaded by the tumor. B, C, D: Sagittal T1-weighted MR image of the left superior sulcus show tumor extension into T1-2 neurovertebral foramen (*).

Radiologist is more confident with MRI for extension evaluation of the tumors within the superior sulcus.

Abbreviations: AS: Anterior scalene muscle, PS: Posterior scalene muscle.

*Meeting "Lung Cancer Imaging in 2012: Updates and innovations", Tervuren, 10.11.2012.
1. Radiology Department, Tenon Hospital, Paris, 2. CNRS UMR 7241/INSERM U1050, Early Development and Pathologies Center for Interdisciplinary Research in Biology, Collège de France, Paris, 3. University of Pierre et Marie Curie, Paris VI, Paris, France.

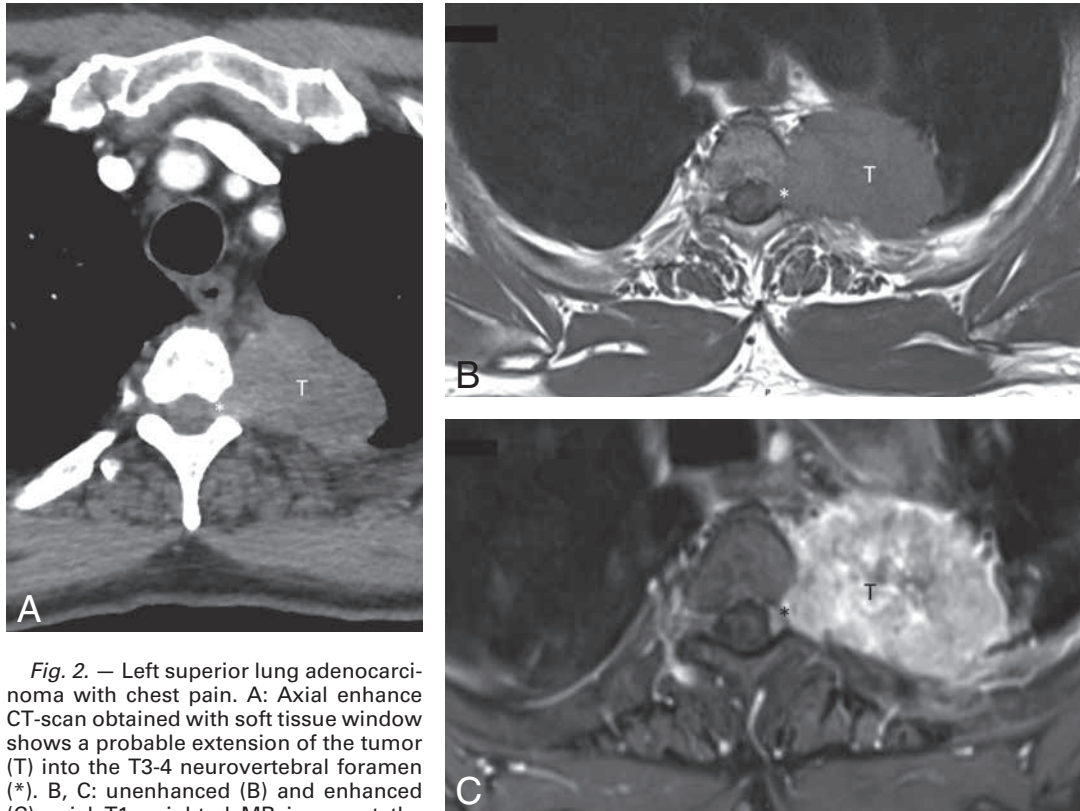


Fig. 2. — Left superior lung adenocarcinoma with chest pain. A: Axial enhance CT-scan obtained with soft tissue window shows a probable extension of the tumor (T) into the T3-4 neurovertebral foramen (*). B, C: unenhanced (B) and enhanced (C) axial T1-weighted MR image at the same level as (A) helps confirm that the mass (T) extends into the T3-4 neurovertebral foramen (*).

MRI are made around the tumor functional exploration including a whole body exploration. This functional exploration focuses on the specific cellular and vascular architecture of tumors using MRI spectroscopy, perfusion MRI and diffusion-weighted images (DWI). The image contrast of DWI is based on the diffusion properties of water molecules and reflects tissue parameters like cellular density especially in tumor and tissue architecture (5). In the last few years, DWI has been investigated successfully in many fields of oncology (6).

In this review we present the contribution of MRI in lung cancer staging including the validated indications and the current development especially with DWI.

Validated indication of MRI in lung cancer staging

In the initial staging, MRI is the gold standard in the detection of brain metastases and the chest wall invasion especially of the superior sulcus tumor (7). It is also recommended in cases of suspected vertebral or epidural localization and in

the characterization of suspected lesions of liver and adrenal.

Superior sulcus tumor

MRI advantages in the evaluation of superior sulcus tumor and determining their resectability include multiplanar capabilities, superior contrast resolution (compared with the other modalities), and lack of ionizing radiation (Fig. 1). MRI is superior to CT in the visualization of tumor extension to the chest wall, extending into the foramina and spinal canal, and the involvement of the brachial plexus (8-11). Although tumor invasion of these structures can be inferred scan data in many cases, MRI allows direct representation of participation and thus improve reader confidence (10). Disadvantages of MRI include its limited availability compared to that of CT, as well as longer time image acquisition and increased sensitivity to motion artifacts and patient claustrophobia. There have been a limited number of prospective studies, conducted in the late 1980s and early 1990s, with small number of patients in which the relative merits of CT and MR imaging of the superior sulcus were

compared (10-12). MRI in all these studies was superior to CT for the assessment of brachial plexus invasion related to the multiplanar MR imaging and contrast resolution. No data are available comparing multidetector CT and MR (7).

MR imaging of superior sulcus tumors is performed by using a protocol described by Bruzzi et al. (7) using a modification of a previous protocol described by Demondion et al. (13, 14). This protocol includes axial, sagittal, and coronal T1-weighted sequences and sagittal T2-weighted sequence. To optimize sensitivity for the small structures in the thoracic inlet, such as the brachial plexus nerve roots and trunks, imaging is performed by using a neurovascular neck coil. T1-weighted sequences are acquired by using thin section (3.0 mm) with a minimal gap (< 0.3 mm) and both cardiac gating and respiratory triggering are used to minimize motion and pulsation artifact. Sagittal T1-weighted sequences provide the most detailed anatomic information and should be performed first in case imaging has to be interrupted or aborted, because the sagittal images alone may provide sufficient diagnostic information.

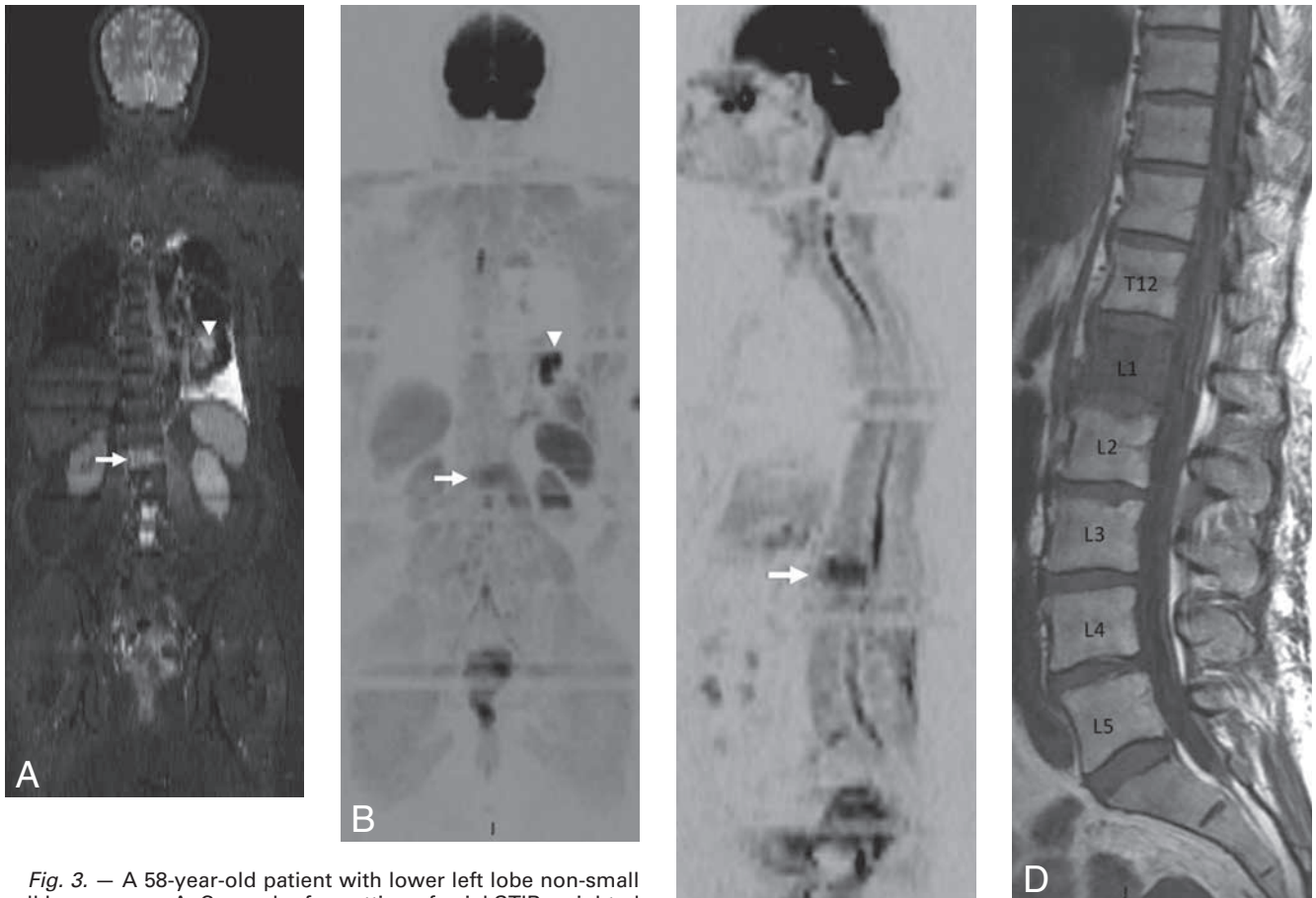


Fig. 3. — A 58-year-old patient with lower left lobe non-small cell lung cancer. A: Coronal reformatting of axial STIR weighted images shows the spinal metastasis (arrow), the lower left lobe tumor (arrowhead) and the left pleural effusion. B, C: Coronal (B) and sagittal (C) reformatting of axial diffusion-weighted images ($b = 1000 \text{ sec/mm}^2$) show with a more marked way the abnormality of signal intensity of the spine and the left lower lobe tumor. D: Sagittal T1-weighted image of the lumbar spine shows clearly the L1 spine involvement by the metastasis of the non-small lung cancer.

Indications of contrast medium are in patients in whom vascular invasion or intraforaminal extension is suspected to be present (Fig. 2); in patients who have undergone neoadjuvant therapy before a planned resection, in whom posttreatment fibrosis may result in blurring of the intermuscular fat planes and difficulty in visualizing the primary tumor; and in patients in whom a recurrence is suspected after definitive treatment (7).

Brain metastases

MRI of the brain is more sensitive and may be more specific for metastases than CT (15, 16). Cerebral metastases occur commonly in lung cancer, particularly from poorly differentiated tumors and adenocarcinoma. MRI with contrast enhancement is the image technique of

choice (17). It has particular advantages in showing lesions in the posterior fossa and adjacent to the skull. Given its overall higher sensitivity, MRI is therefore currently preferred over CT when screening patients with lung cancer for brain metastases.

Liver metastases

MR imaging with gadolinium chelates offers an accurate non-radiation based imaging test for detection of liver metastases (18). Liver specific MR contrast agents (hepatobiliary and reticuloendothelial agents) offer greater lesion-to-liver contrast than the conventional extracellular agents (gadolinium chelates). Liver specific MR contrast agents may be used in selected clinical situations when the goal is to achieve the highest detection rate for liver focal lesions, for

example, when a patient is being evaluated for curative liver resection (19). The diagnostic performance of DWI is equal to that of Gd-MRI. DWI alone can be used in patients where gadolinium contrast administration is not allowed. Combination of Gd-MRI and DWI significantly increases diagnostic accuracy (20).

Bone metastases

MRI is both sensitive and specific for diagnosing skeletal metastases (Fig. 3), and previous limitations have been overcome with the introduction of whole-body MRI (21, 22).

Adrenal metastases

The discovery of an adrenal gland mass more than 5 cm in the context of lung cancer most often corresponds to a metastatic lesion, except

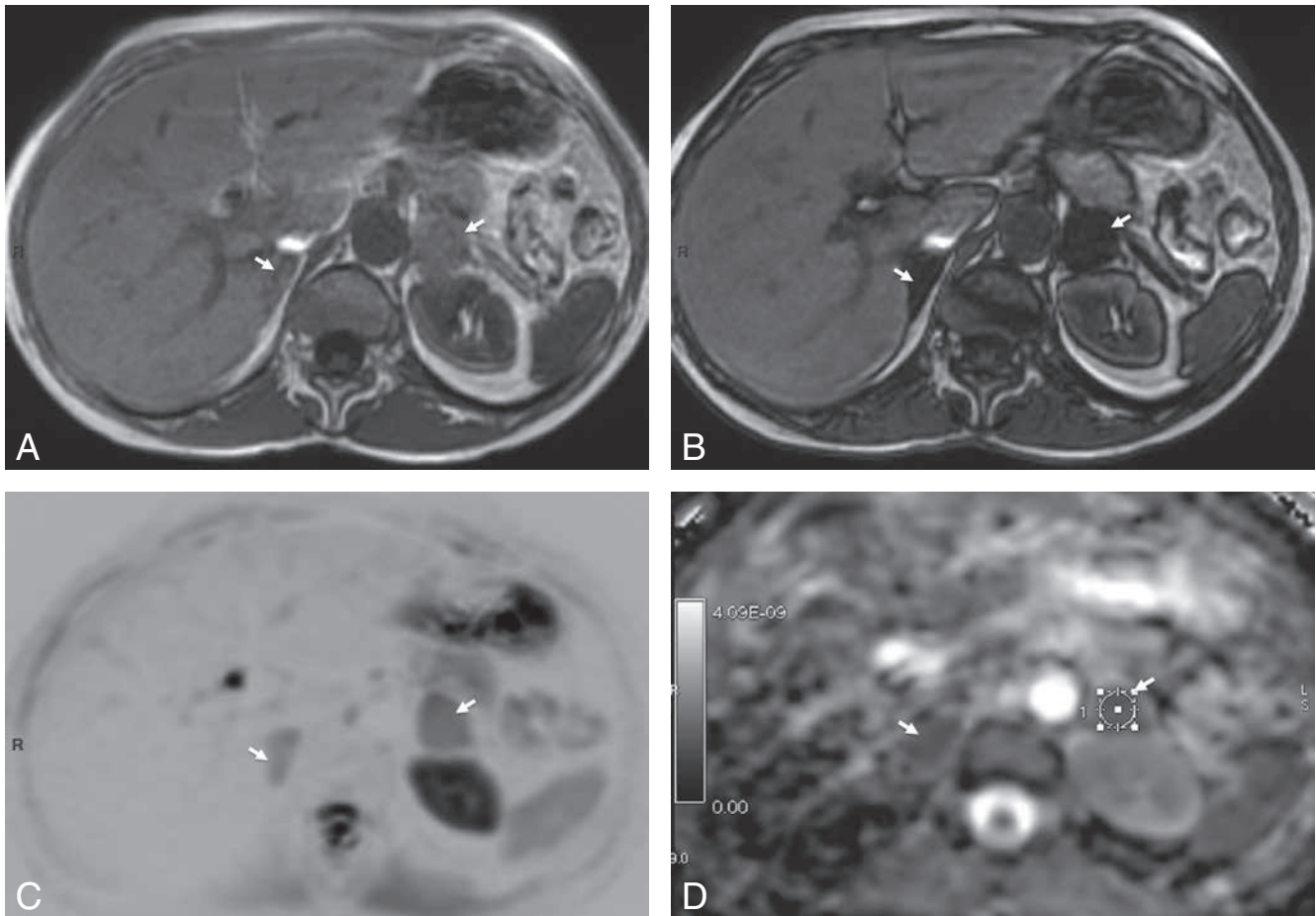


Fig. 4. — Bilateral adrenal adenomas in patient with lung cancer. A: Axial gradient-echo T1-weighted in-phase image shows a bilateral mass of adrenal gland (arrows) in high signal intensity. B: Axial gradient-echo T1-weighted out-phase image shows a strongly decreased signal intensity (arrows) of both adrenal masses related to the presence of a fat component.

C, D: Axial diffusion-weighted images ($b = 1000 \text{ sec/mm}^2$) with inverted grey scale (C) shows a persistence of signal (arrows) on both adrenal glands. The mean ADC value (D) of the left adrenal mass is $1.42 \cdot 10^{-9} \text{ mm}^2/\text{sec}$.

myelolipoma and adrenal cyst, the characteristics of their content, with fat for first and liquid for the second, are easily identified. The problem is especially for small lesions less than 3 cm and having a density enhancement after injection. In most cases, insofar as it is an initial assessment, no previous review is available. The problem of finding these adrenal lesions can be studied by the structural approach in differentiating benign and malignant lesions on the basis of the presence or absence of intracytoplasmic lipids. In benign lesions, lipids are observed, whereas in malignant lesions, the cells containing them are destroyed (Fig. 4). Chemical shift MRI uses a technique based on hydrogen and fat protons, which resonate at different frequencies. By using different time parameters during the same MRI examination, it is possible to identify lipid-rich adenomas. These adenomas show signal loss on out-of-phase imaging, as opposed to im-

aging when the protons are in phase. In contrast, nonadenomas do not show signal loss on out-of-phase imaging (23). Recent studies have shown that 60 to 89 percent of lesions measuring between 10 and 30 HU on unenhanced CT can be characterized using chemical shift MRI (24,25).

Current development of MR in lung cancer

Powered by tremendous advances in image quality over the past few years, diffusion-weighted imaging with or without background signal suppression has drawn strong interest from the radiologic community and major MR vendors. DW imaging is increasingly used in the thorax, particularly in lung nodules and masses, with promising results for lung nodule lesion detection and characterization. DW imaging can be easily implemented in clinical proto-

cols, as it can be performed relatively quickly (as short as two breath-hold acquisitions or during free breathing or with respiratory triggering) and does not require contrast agent injection, which makes it attractive in patients with decreased renal function, who cannot receive gadolinium-based contrast agents. This recent development of DW leads to other promising opportunities than the detection and characterization of pulmonary lesions, such as the initial staging of lung cancer with the TNM staging and to monitor treatment.

Tissues characterization

Tissue characterization in lung nodule or mass, like other organs, stays a challenge even with the development of ^{18}F -FDG PET/CT and the kinetic contrast enhancement using CT or MR. Some DWI MR studies focus on tumor detection and characterization of lung nodules or

Table I. — Sensitivity, specificity, and accuracy of diffusion-weighted imaging on the diagnosis of lung nodules or masses.

Authors	Year	MRI System	Study design	N° of patients	Nodules Malign / Benign	b s/mm ²	Cutoff	Sensibility (95% CI)	Specificity (95% CI)	Accuracy (95% CI)
Mori et al. (27)	2008	Achieva	Prospective	114	106/34	0 / 1000	1.1	0.7 (0.6-0.79)	0.97 (0.84-1.00)	0.76 (0.69-0.84)
Satoh et al. (30)	2008	Intera	Retrospective Consecutive	51	36/18	0 / 1000	ND	0.89 (0.74-0.97)	0.61 (0.36-0.83)	0.80 (0.69-0.90)
Ohba et al. (29)	2009	Achieva	Retrospective Consecutive	110	96/28	0 / 1000	1.2	0.84 (0.74-0.91)	0.93 (0.68-1.00)	0.78 (0.71-0.85)
Uto et al. (33)	2009	Signa	Prospective	28	18/10	0 / 1000	0.834	0.72 (0.47-0.90)	0.10 (0.00-0.45)	0.5 (0.42-0.68)
Liu et al. (26)	2010	Twin-Speed Infinity	Retrospective Consecutive	62	54/12	0 / 500	1.4	0.83 (0.69-0.92)	0.74 (0.45-0.92)	0.7 (0.59-0.81)
Ohba et al. (28)	2011	Achieva (1.5T)	Prospective	58	58/18	0 / 1000	1	0.91 (0.84-0.99)	0.94 (0.83-1.00)	0.92 (0.86-0.98)
Ohba et al. (28)	2011	Achieva (3T)	Prospective	58	58/18	0 / 1000	1.85	0.90 (0.82-0.98)	0.94 (0.83-1.00)	0.91 (0.85-0.97)
Tondo et al. (32)	2011	Achieva	Retrospective	34	30/4	0 / 500 / 1000	1.25	0.90 (0.73-0.98)	1.00 (0.40-1.00)	0.91 (0.82-1.00)
Sommer et al. (31)	2012	Avanto	Prospective	31	28 / 3	0 / 800	ND	0.93 (0.84-1.00)	0.5 (0-0-1.00)	0.89 (0.77-1.00)

masses (26-33) (Table I). MR is as accurate as ¹⁸F-FDG PET/CT for nodule or masses characterization (Fig. 5). MR is more specific comparing to ¹⁸F-FDG PET/CT in characterization of lung masses or mediastinal lymphadenopathies. In a recent meta-analysis on nodule or mass characterization Wu et al, confirm this assessment on showing that DWI is useful for differentiation between malignant and benign pulmonary nodules with pooled sensitivity of 0.84 and specificity of 0.84. Large-scale randomized controlled trials are still necessary to assess and confirm its clinical value. A threshold value for malignant/benign lesion classification could not be made based on this study because it is influenced by different b values, bias of patient selection, lesions' pathological characteristics and ADC measurement. Selection of the threshold value should be determined according to the purpose of examination. A relatively higher threshold value may be recommended to minimize missing malignancy in lung cancer screening. If DWI is appended to other diagnostic method (e.g., computed tomography), a relatively lower threshold value may be recommended to reduce false-positive results.

To go further in the characterization, Matoba et al. (34) reported the ADC value of lung cancer based on its histological type. This study covers only 30 lesions. ADC values of the means were 2.12+/-0.6 10⁻³mm²/sec (adenocarcinoma), 1.63+/-0.5 10⁻³mm²/sec (squamous cell carcinoma), 1.3+/-0.4 10⁻³mm²/sec (large cell carcinoma) and 2.09+/-0.3 10⁻³mm²/sec (small cell carcinoma) The value of the ADC adenocarcinomas was significantly higher than that of squamous cell carcinomas and large cell carcinomas (p < 0.05). In addition to the value of the ADC well-differentiated adenocarcinomas (2.52+/-0.4 10⁻³mm²/sec) was significantly higher than that of poorly differentiated adenocarcinoma and squamous cell carcinoma.

DWI has its place in some special situations to reduce the failure of transthoracic biopsy for large partially necrotic masses (direct biopsy area to which the cell density is highest, the lowest ADC) and differentiates atelectasis from tumor to show the target biopsy (Fig. 6). In the latter situation the DWI is more accurate than other sequences including T2-weighted normal (35). MRI always keeps a place in the characterization of silicotic nodules of patients exposed to silica with no signal on T2-

weighted and diffusion while these nodules are associated with a high uptake in ¹⁸F-FDG PET/CT with SUV value greater than 10.

Mediastinal and hilar nodal staging

In patients with NSCLC, involvement of the mediastinal lymph nodes is an important prognostic factor because accurate disease staging is needed to limit surgery or multimodality treatment to only of those who might benefit from such treatment (Fig. 7). A recent meta-analysis (36) comparing ¹⁸F-FDG PET/CT to DWI showed that DWI has a high specificity for N staging of NSCLC compared with ¹⁸F-FDG PET/CT and has the potential to be a reliable alternative noninvasive imaging method for the preoperative staging of mediastinal and hilar lymph node in patients with NSCLC (37-41). However, they believe it is too early to call for broad application of this method in clinical practice. They speculate that additional improvement of the technology will increase its role in the future. Additional, larger, prospective, directly comparative studies involving ¹⁸F-FDG PET/CT would be required to determine the true value of DWI for the diagnosis of lymph node metastasis in patients with NSCLC.

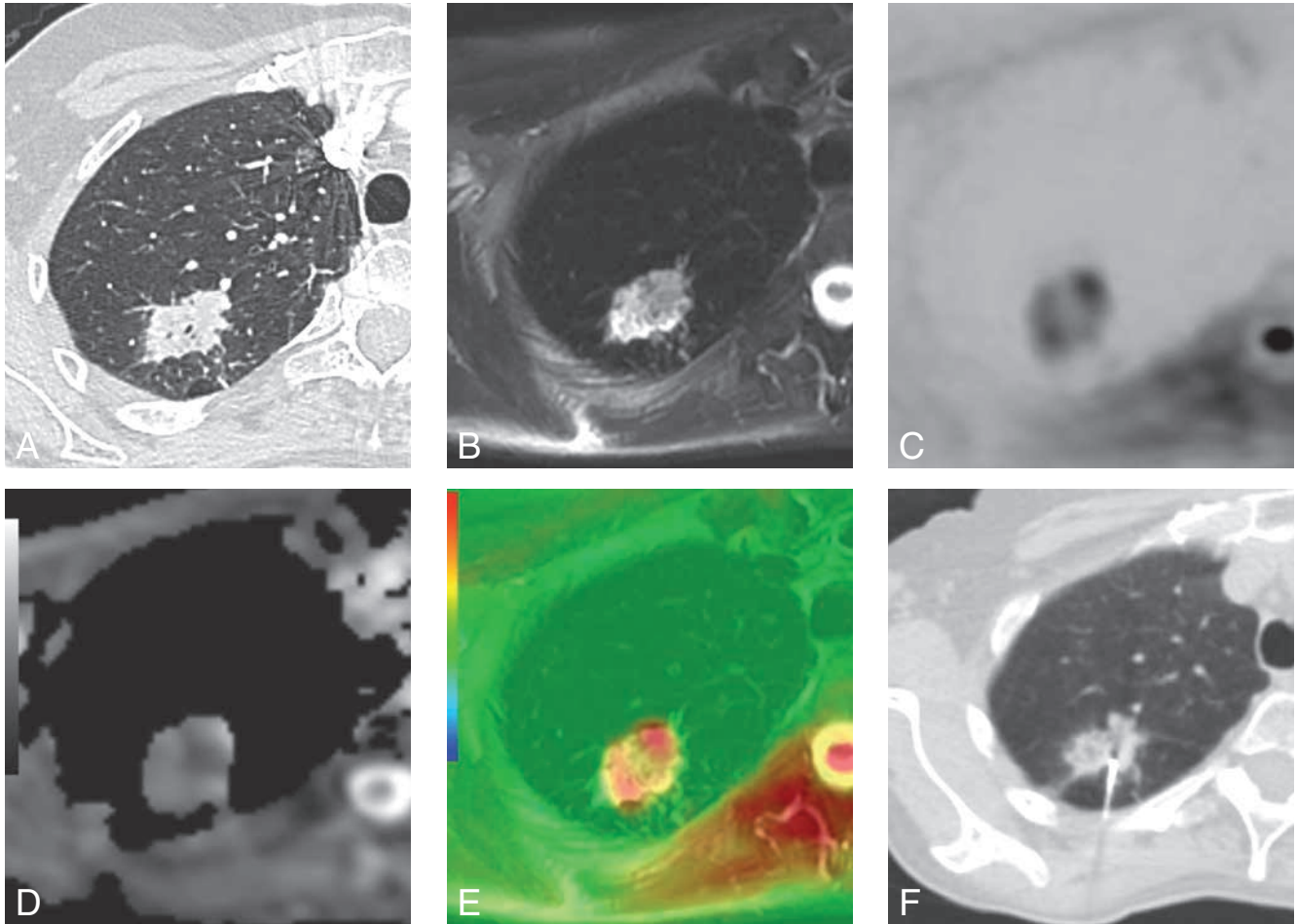


Fig. 5. — Right upper lobe alveolar nodule in a 58-year-old smoker woman. A: Axial CT-scan on parenchymal window shows the alveolar nodule with spiculated margins. B- Axial TSE T2-weighted Fat sat with the PROPELLER technique image with respiratory-gated shows clearly the nodule with high signal intensity and spiculated margins. C, D: Axial diffusion-weighted images ($b = 1000 \text{ sec/mm}^2$) with inverted grey scale (C) shows higher signal on the periphery. The mean ADC value (D) on the periphery is $1.13 \cdot 10^{-9} \text{ mm}^2/\text{sec}$. E- Fusion of both axial images of the TSE T2-weighted Fat sat with the PROPELLER technique and the diffusion-weighted image ($b = 1000 \text{ sec/mm}^2$) shows the exact location of the high cellular area. F- Trans-thoracic needle biopsy directed toward the highest cell density area diagnoses an adenocarcinoma.

Table II. — Sensitivity, specificity, and accuracy of diffusion-weighted imaging on the mediastinal and hilar nodal staging.

Authors	Year	MRI System	Study design	N° of patients	Lymph nodes Malign / Benign	b s/mm ²	Cutoff	Sensibility (95% CI)	Specificity (95% CI)	Accuracy (95% CI)
Hasegawa et al. (37)	2008	Achieva	Prospective	42	5/37	0 / 1000	ND	0.8 (0.68-0.92)	0.97 (0.92-1.03)	0.95 (0.87-1.02)
Nomori et al. (31, 39)	2008	Intera	Prospective	88	36/698	0 / 1000	1.6	0.67 (0.52-0.82)	0.99 (0.98-1.0)	0.98 (0.97-0.98)
Nakayama et al. (38)	2010	Avanto	Retrospective	70	13/54	50 / 1000	ND	0.69 (0.58-0.80)	1	0.94 (0.88-1.0)
Chen et al. (42)	2010	Avanto	Retrospective Consecutive	56	97/38	0 / 1000	ND	0.91 (0.87-0.95)	0.90 (0.85-0.96)	0.9 (0.85-0.96)
Ohno et al. (40)	2011	Achieva	Prospective	250	157/93	0 / 1000	2.5	0.75 (0.7-0.8)	0.87 (0.84-0.91)	0.81 (0.75-0.86)
Usuda et al. (41)	2011	Avanto	Prospective	63	44/275	0 / 800	1.7	0.75 (0.71-0.79)	0.99 (0.98-1.0)	0.95 (0.93-0.97)
Sommer et al. (31)	2012	Avanto	Prospective	31	28 / 3	0 / 800	ND	0.44 (0.19-0.68)	0.93 (0.87-0.99)	0.85 (0.72-0.97)

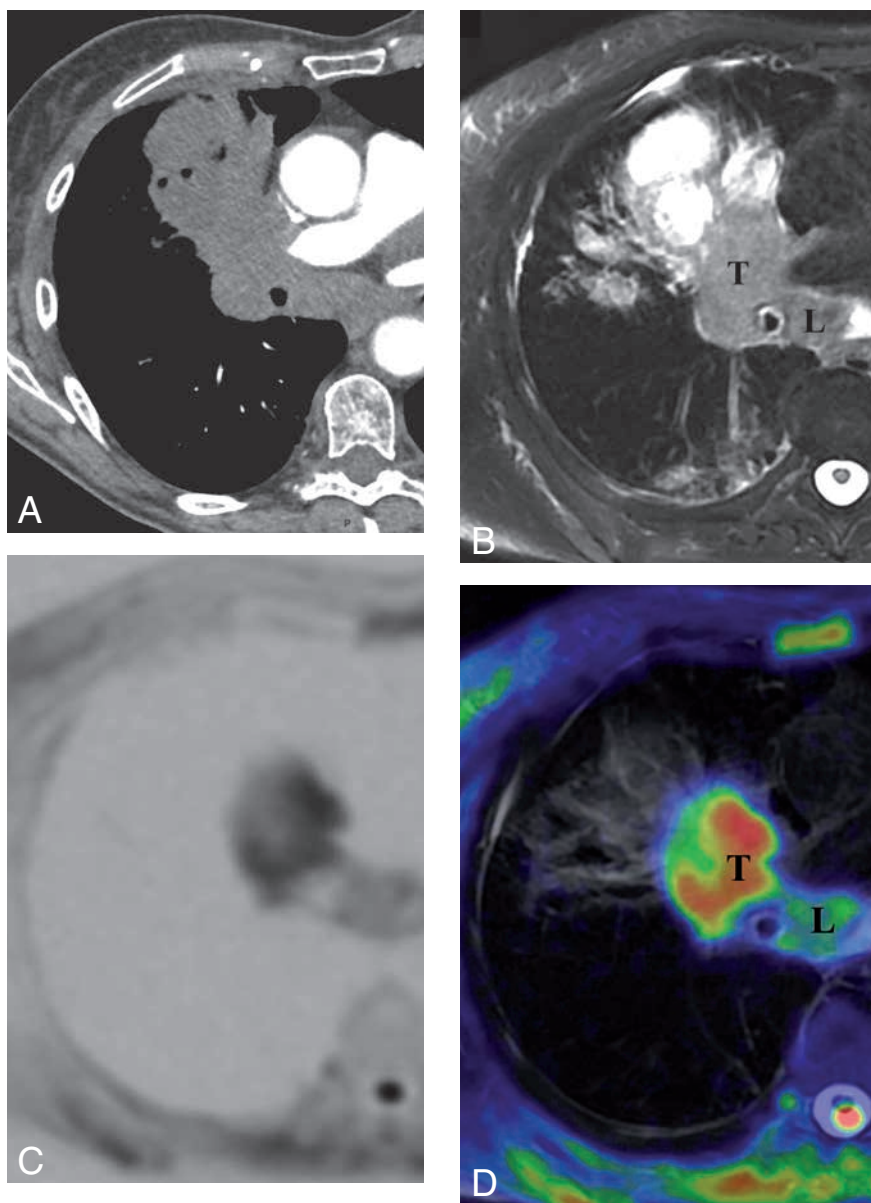


Fig. 6. — Right upper lobe mass in a 62-year-old woman. A: Axial enhanced CT scan shows the tumor (T) and sub-carinal lymphadenopathies (L). B: Axial T2-weighted TSE image with fat suppression and with the PROPELLER technique and respiratory-gated shows the tumor (T), the lymphadenopathy (L), and probably an obstructive pneumonitis. C: Axial diffusion-weighted images ($b = 1000 \text{ sec/mm}^2$) with inverse grey scale for lung collapse and obstructive pneumonia. D: Fusion of both axial images of the TSE T2-weighted Fat sat with the PROPELLER technique and the diffusion-weighted image ($b = 1000 \text{ sec/mm}^2$) shows the exact location of the high cellular area related to the tumor process.

Nomori et al. (39) reported that the accuracy of N staging in 88 patients was 0.89 with DWI, significantly greater than the value of 0.78 obtained with ^{18}F -FDG PET/CT because of less overstaging in the former. The superiority of DWI can be explained by the observation that not only did DWI give fewer false-positive results for N staging of NSCLC

than did ^{18}F -FDG PET/CT (39), but also DWI gave fewer false-negative results for N staging of NSCLC than did ^{18}F -FDG PET/CT. ^{18}F -FDG PET/CT is likely to show false positive results when lymph nodes contain inflammation and is likely to show false-negative results when the lymph nodes contain a small amount of cancer cells. The DWI with an ADC

value and signal intensity can be useful in the differentiation of malignant and benign mediastinal lymph nodes (39). DWI can be used in place of ^{18}F -FDG PET/CT for N staging of NSCLC, especially in hospitals in which MRI examinations can be done but ^{18}F -FDG PET/CT examinations cannot.

M staging with Whole body MR including DWI

Ohno et al. (21) prospectively compared whole-body DWI alone, whole-body DWI combined with conventional whole-body MRI, and ^{18}F -FDG PET/CT for M-stage assessment in 203 NSCLC patients. The final M-stage and metastasis of a given site were determined on the basis of the results of conventional radiologic, ^{18}F -FDG PET/CT, and whole-body MRI examinations and on the basis of pathologic results from endoscopic, CT-guided, or surgical biopsies, as well as on the basis of the results of follow-up examinations performed on every patient for more than 12 mo. The area under the ROC curve of whole-body DWI (0.79) was significantly lower ($P < 0.05$) than that of ^{18}F -FDG PET/CT (0.89). However, the area under the curve of whole-body DWI combined with conventional whole-body MRI (0.87) was not significantly different from that of ^{18}F -FDG PET/CT. The authors concluded that whole-body MRI with DWI can be used for M-stage assessment in patients with NSCLC with accuracy (area under the curve, 0.87) as good as that of ^{18}F -FDG PET/CT (area under the curve, 0.89).

In a more recent study of Chen et al. (42), 62 lesions were considered as metastases based on initial findings, 37 distant metastatic lesions (brain, three; liver, six; adrenal gland, two; and bone, 26) and six lung metastatic lesions were validated by biopsy or radiologic follow-up. A total of 35 distant metastases were detected based on DWI. Three lesions of lung metastases, sized less than 10 mm, were not detected at DWI; there was one false-positive bone lesion with DWI. Meanwhile, 37 distant metastases were detected with ^{18}F -FDG PET/CT; five lung metastatic lesions were detected by ^{18}F -FDG PET/CT. Only one lung metastatic lesion was missed and no false-positive result at ^{18}F -FDG PET/CT. DWI was found to be sensitive in osseous metastasis. The sensitivity, specificity, positive predictive value, negative predictive value and accuracy for detection of metastasis for DWI

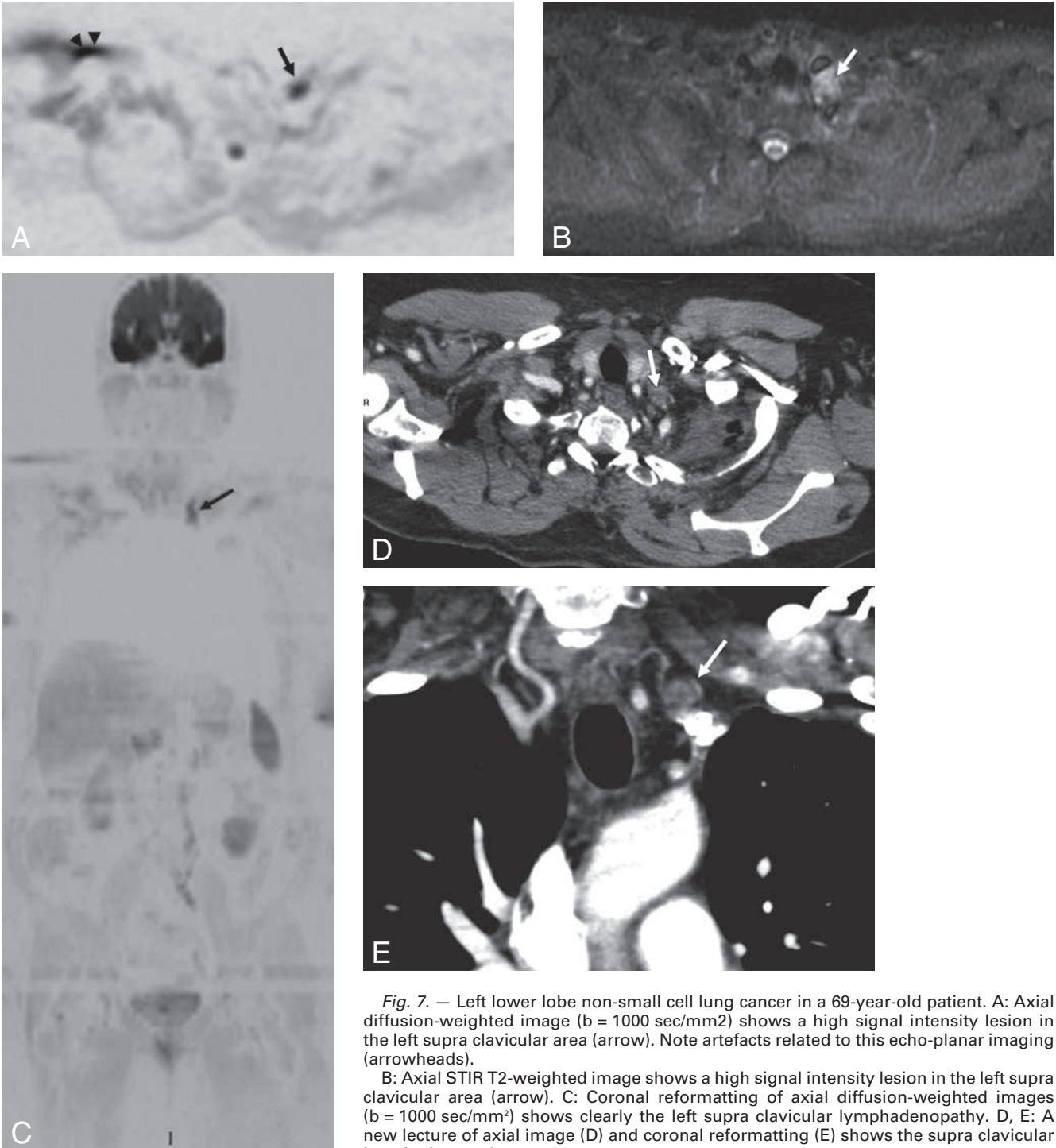


Fig. 7. — Left lower lobe non-small cell lung cancer in a 69-year-old patient. A: Axial diffusion-weighted image ($b = 1000 \text{ sec/mm}^2$) shows a high signal intensity lesion in the left supraclavicular area (arrow). Note artefacts related to this echo-planar imaging (arrowheads).

B: Axial STIR T2-weighted image shows a high signal intensity lesion in the left supraclavicular area (arrow). C: Coronal reformatting of axial diffusion-weighted images ($b = 1000 \text{ sec/mm}^2$) shows clearly the left supraclavicular lymphadenopathy. D, E: A new lecture of axial image (D) and coronal reformatting (E) shows the supraclavicular lymphadenopathy.

were 0.9; 0.95; 0.97; 0.83 and 0.92 respectively. The sensitivity, specificity, positive predictive value, negative predictive value and accuracy for detection of metastasis for integrated ^{18}F -FDG PET/CT were 0.98, 1; 1; 0.95 and 0.98 respectively.

Conclusion

Major advances in the WB-MRI in the initial evaluation and follow-up of patients with lung cancer have been performed in recent years. Multicentric studies using different mag-

net systems are necessary to confirm these promising results. One thing is certain, for metastatic and lymph node staging, that whole-body MRI with the information obtained by WB-DWI and WB-MRI is greater than the scanner including staging and

lymph node metastasis. Data comparing MRI whole body PET-CT are rare. The implementation of this technique requires a thorough knowledge of MRI, including the management of artifacts generated by echo-planar sequence.

References

1. Ferlay J., Parkin D.M., Steliarova-Foucher E.: Estimates of cancer incidence and mortality in Europe in 2008. *Eur J Cancer*, 2010, 46: 765-81.
2. Siegel R., Ward E., Brawley O., Jemal A.: Cancer statistics, 2011: the impact of eliminating socioeconomic and racial disparities on premature cancer deaths. *CA: a cancer journal for clinicians*, 2011, 61: 212-236.
3. Aquino S.L., Kuester L.B., Muse V.V., Halpern E.F., Fischman A.J.: Accuracy of transmission CT and FDG-PET in the detection of small pulmonary nodules with integrated PET/CT. *Eur J Nucl Med and Mol Imag*, 2006, 33: 692-696.
4. Roberts P.F., Follette D.M., von Haag D., Park J.A., Valk P.E., Pounds T.R., et al.: Factors associated with false-positive staging of lung cancer by positron emission tomography. *Ann Thorac Surg*, 2000, 70: 1154-1159.
5. Koh D.M., Collins D.J.: Diffusion-weighted MRI in the body: applications and challenges in oncology. *AJR*, 2007, 188: 1622-1635.
6. Padhani A.R., Koh D.M., Collins D.J.: Whole-body diffusion-weighted MR imaging in cancer: current status and research directions. *Radiology*, 2011, 261: 700-718.
7. Bruzzi J.F., Komaki R., Walsh G.L., Truong M.T., Gladish G.W., Munden R.F., et al.: Imaging of non-small cell lung cancer of the superior sulcus: part 2: initial staging and assessment of resectability and therapeutic response. *Radiographics*, 2008, 28: 561-572.
8. Takasugi J.E., Rapoport S., Shaw C.: Superior sulcus tumors: the role of imaging. *J Thorac Imag.*, 1989, 4: 41-48.
9. Beale R., Slater R., Hennington M., Keagy B.: Pancoast tumor: use of MRI for tumor staging. *South Med J*, 1992, 85: 1260-1263.
10. Heelan R.T., Demas B.E., Caravelli J.F., Martini N., Bains M.S., McCormack P.M., et al.: Superior sulcus tumors: CT and MR imaging. *Radiology*, 1989, 170: 637-641.
11. Rapoport S., Blair D.N., McCarthy S.M., Desser T.S., Hammers L.W., Sostman H.D.: Brachial plexus: correlation of MR imaging with CT and pathologic findings. *Radiology*, 1988, 167: 161-165.
12. Iezzi A., Magarelli N., Carriero A., Podda P.F., Ciccotosto C., Bonomo L.: Staging of pulmonary apex tumors. Computerized tomography versus magnetic resonance. *Radiologia Med*, 1994, 88: 24-30.
13. Demondion X., Bacqueville E., Paul C., Duquesnoy B., Hachulla E., Cotten A.: Thoracic outlet: assessment with MR imaging in asymptomatic and symptomatic populations. *Radiology*, 2003, 227: 461-468.
14. Demondion X., Boutry N., Drizenko A., Paul C., Francke J.P., Cotten A.: Thoracic outlet: anatomic correlation with MR imaging. *AJR*, 2000, 175: 417-422.
15. Sze G., Shin J., Krol G., Johnson C., Liu D., Deck M.D.: Intraparenchymal brain metastases: MR imaging versus contrast-enhanced CT. *Radiology*, 1988, 168: 187-194.
16. Yokoi K., Kamiya N., Matsuguma H., Machida S., Hirose T., Mori K., et al.: Detection of brain metastasis in potentially operable non-small cell lung cancer: a comparison of CT and MRI. *Chest*, 1999, 115: 714-719.
17. Sze G., Johnson C., Kawamura Y., Goldberg S.N., Lange R., Friedland R.J., et al.: Comparison of single- and triple-dose contrast material in the MR screening of brain metastases. *AJNR*, 1998, 19: 821-828.
18. Namasivayam S., Martin D.R., Saini S.: Imaging of liver metastases: MRI. *Cancer Imag*, 2007, 7: 2-9.
19. Morana G., Cugini C., Mucelli R.P.: Small liver lesions in oncologic patients: characterization with CT, MRI and contrast-enhanced US. *Cancer Imag*, 2008, 8 Spec No A: S132-13.
20. Kenis C., Deckers F., De Foer B., Van Mieghem F., Van Laere S., Pouillon M.: Diagnosis of liver metastases: can diffusion-weighted imaging (DWI) be used as a stand alone sequence? *Eur J Radiol*, 2012, 81: 1016-1023.
21. Ohno Y., Koyama H., Onishi Y., Takenaka D., Nogami M., Yoshikawa T., et al.: Non-small cell lung cancer: whole-body MR examination for M-stage assessment – utility for whole-body diffusion-weighted imaging compared with integrated FDG PET/CT. *Radiology*, 2008, 248: 643-654.
22. Takenaka D., Ohno Y., Matsumoto K., Aoyama N., Onishi Y., Koyama H., et al.: Detection of bone metastases in non-small cell lung cancer patients: comparison of whole-body diffusion-weighted imaging (DWI), whole-body MR imaging without and with DWI, whole-body FDG-PET/CT, and bone scintigraphy. *J Magn Reson Imaging*, 2009, 30: 298-308.
23. Israel G.M., Korobkin M., Wang C., Hecht E.N., Krinsky G.A.: Comparison of unenhanced CT and chemical shift MRI in evaluating lipid-rich adrenal adenomas. *AJR*, 2004, 183: 215-219.
24. Haider M.A., Ghai S., Jhaveri K., Lockwood G.: Chemical shift MR imaging of hyperattenuating (> 10 HU) adrenal masses: does it still have a role? *Radiology*, 2004, 231: 711-716.
25. Yoh T., Hosono M., Komeya Y., Im S.W., Ashikaga R., Shimono T., et al.: Quantitative evaluation of norcholesterol scintigraphy, CT attenuation value, and chemical-shift MR imaging for characterizing adrenal adenomas. *Ann Nucl Med*, 2008, 22: 513-519.
26. Liu H., Liu Y., Yu T., Ye N.: Usefulness of diffusion-weighted MR imaging in the evaluation of pulmonary lesions. *Eur Radiol*, 2010, 20: 807-815.
27. Mori T., Nomori H., Ikeda K., Kawanaka K., Shiraishi S., Katahira K., et al.: Diffusion-weighted magnetic resonance imaging for diagnosing malignant pulmonary nodules/masses: comparison with positron emission tomography. *J Thorac Oncol*, 2008, 3: 358-364.
28. Ohba Y., Nomori H., Mori T., Shiraishi K., Namimoto T., Katahira K.: Diffusion-weighted magnetic resonance for pulmonary nodules: 1.5 vs. 3 Tesla. *Asian Cardiovascular Thorac Ann*, 2011, 19: 108-114.
29. Ohba Y., Nomori H., Mori T., Ikeda K., Shibata H., Kobayashi H., et al.: Is diffusion-weighted magnetic resonance imaging superior to positron emission tomography with fludeoxyglucose F 18 in imaging non-small cell lung cancer? *J Thorac Cardiovasc Surg*, 2009, 138: 439-445.
30. Satoh S., Kitazume Y., Ohdama S., Kimura Y., Taura S., Endo Y.: Can malignant and benign pulmonary nodules be differentiated with diffusion-weighted MRI? *AJR*, 2008, 191: 464-470.
31. Sommer G., Wiese M., Winter L., Lenz C., Klarhofer M., Forrer F., et al.: Preoperative staging of non-small-cell lung cancer: comparison of whole-body diffusion-weighted magnetic resonance imaging and (18)F-fluorodeoxyglucose-positron emission tomography/computed tomography. *Eur Radiol*, 2012, 22: 2859-2867.
32. Tondo F., Saponaro A., Stecco A., Lombardi M., Casadio C., Carriero A.: Role of diffusion-weighted imaging in the differential diagnosis of benign and malignant lesions of the chest-mediastinum. *Radiologia Med*, 2011, 116: 720-733.
33. Uto T., Takehara Y., Nakamura Y., Naito T., Hashimoto D., Inui N., et al.: Higher sensitivity and specificity for diffusion-weighted imaging of malignant lung lesions without apparent diffusion coefficient quantification. *Radiology*, 2009, 252: 247-254.
34. Matoba M., Tonami H., Kondou T., Yokota H., Higashi K., Toga H., et al.: Lung carcinoma: diffusion-weighted mr imaging--preliminary evaluation with apparent diffusion coefficient. *Radiology*, 2007, 243: 570-577.
35. Qi L.P., Zhang X.P., Tang L., Li J., Sun Y.S., Zhu G.Y.: Using diffusion-weighted MR imaging for tumor detection in the collapsed lung: a preliminary study. *Eur Radiol*, 2009, 19: 333-341.
36. Wu L.M., Xu J.R., Gu H.Y., Hua J., Chen J., Zhang W., et al.: Preoperative mediastinal and hilar nodal staging with diffusion-weighted magnetic resonance imaging and fluorodeoxyglucose positron emission tomography/computed tomography in patients with non-small-cell lung cancer: Which is better? *J Surg Research*, 2012, 178: 304-314.
37. Hasegawa I., Boiselle P.M., Kuwabara K., Sawafuji M., Sugiura H.: Mediastinal lymph nodes in patients with non-small cell lung cancer: preliminary experience with diffusion-weighted MR imaging. *J Thorac Imag*, 2008, 23: 157-161.

38. Nakayama J., Miyasaka K., Omatsu T., Onodera Y., Terae S., Matsuno Y., et al.: Metastases in mediastinal and hilar lymph nodes in patients with non-small cell lung cancer: quantitative assessment with diffusion-weighted magnetic resonance imaging and apparent diffusion coefficient. *J Comput Assist Tomogr*, 2010, 34: 1-8.
39. Nomori H., Mori T., Ikeda K., Kawanaka K., Shiraishi S., Katahira K., et al.: Diffusion-weighted magnetic resonance imaging can be used in place of positron emission tomography for N staging of non-small cell lung cancer with fewer false-positive results. *J Thorac Cardiovasc Surg*, 2008, 135: 816-822.
40. Ohno Y., Koyama H., Yoshikawa T., Nishio M., Aoyama N., Onishi Y., et al.: N stage disease in patients with non-small cell lung cancer: efficacy of quantitative and qualitative assessment with STIR turbo spin-echo imaging, diffusion-weighted MR imaging, and fluorodeoxyglucose PET/CT. *Radiology*, 2011, 261: 605-615.
41. Usuda K., Zhao X.T., Sagawa M., Matoba M., Kuginuki Y., Taniguchi M., et al.: Diffusion-weighted imaging is superior to positron emission tomography in the detection and nodal assessment of lung cancers. *Ann Thorac Surg*, 2011, 91: 1689-1695.
42. Chen W., Jian W., Li H.T., Li C., Zhang Y.K., Xie B., et al.: Whole-body diffusion-weighted imaging vs. FDG-PET for the detection of non-small-cell lung cancer. How do they measure up? *Magn Reson Imaging*, 2010, 28: 613-620.

Take advantage of our pre-publication offer:

Andreas Vesalius: The Fabric of the Human Body
(Annotated Translation of the 1543 and 1555 editions of "De Humani Corporis Fabrica")

Publication date: October 2013.
Subscribe now at introductory pricing: 890 EUR
(normal price 1320 EUR)

The book is published in two volumes, in cassette, in the original Full Foolscap format (432 x 343 mm).

More information: www.acco.be/vesalius

ACCO Leuven M-Theresiastraat 2 3000 Leuven Tel 016/29.11.00 Fax 016/20.73.89	ACCO Adréline 43, Rue Martin V 1200 Bruxelles Tel 02/763.16.86 Fax 02/772.10.04	ACCO Gent St-Pietersnieuwstr. 105 9000 Gent Tel 09/235.73.00 Fax 09/235.73.01
--	---	---

acco.medical@acco.be
www.accomedical.be